^{2}H nuclear magnetic resonance studies on the deuteron dynamics in betaine phosphate/phosphite mixed crystals

1999 J. Phys.: Condens. Matter 11 1575

(http://iopscience.iop.org/0953-8984/11/6/022)

J. Phys.: Condens. Matter **11** (1999) 1575–1588. Printed in the UK PII: S0953-8984(99)97973-0

^{2}H nuclear magnetic resonance studies on the deuteron dynamics in betaine phosphate/phosphite mixed crystals

J Totz, H Braeter and D Michel

Universität Leipzig, Fakultät für Physik und Geowissenschaften, Linnéstraße 5, D-04103 Leipzig, Germany

Received 29 September 1998, in final form 13 November 1998

Abstract. One- and two-dimensional ^{2}H NMR measurements on selected single crystals of deuterated betaine phosphate/phosphite mixed crystals ($DBP_{1-x}DBPI_x$) in the antiferrodistortive and paraelectric phases were performed in order to study the static and dynamic behaviour of the deuterium atoms in the hydrogen bridges and in the methylene groups.

In the ^{2}H nuclear magnetic resonance (NMR) spectra of the mixed crystals, it is possible to distinguish between DBP and DBPI molecules. Furthermore, for all deuterons the electric field gradient (EFG) tensors could be determined. A characteristic dependency of the high-temperature phase transition on the phosphite concentration x was derived from the changes of the one-dimensional ^{2}H NMR spectra. Our suggested model, which describes this dependency qualitatively, underlines the antiferrodistortive character of this transition. Furthermore, from the line-shape variations, the occurrence of processes of exchange between several deuterons, including DBP *and* DBPI molecules, was concluded. The presence of exchange between *different* molecules in the chains was confirmed by means of analysing the cross-peaks of two-dimensional ^{2}H NMR exchange experiments. The observation of this charge-transport process along the chains from the microscopic point of view is very important for the understanding of electrical conductivity processes in these crystals.

1. Introduction

Betaine phosphate ($(CH_3)_3NCH_2COOH_3PO_4$), betaine phosphite ($(CH_3)_3NCH_2COOH_3PO_3$) (which are abbreviated as BP and BPI), and the respective deuterated compounds (DBP and DBPI), as well as the mixed-crystal system $DBP_{1-x}DBPI_x$, belong to a group of crystals which are each composed of the amino acid betaine and an inorganic component. These crystals are, together with other ferroelectrics which also contain hydrogen bonds, considered model substances for the study of phase behaviour and structural phase transitions. In recent years, the mixed crystals $DBP_{1-x}DBPI_x$ have been of particular interest because of their competing ferroelectric and antiferroelectric interactions.

BP and BPI each undergo a structural phase transition from a paraelastic (pe) high-temperature phase to an antiferrodistortive (afd) phase—at 365 K [1] and 355 K [2], respectively—which is almost unchanged by deuteration. Each crystal possesses a monoclinic structure ($P2_1/c$) with four formula units per unit cell. Below 86 K, an antiferroelectric ordering occurs in BP, whereas in BPI, a ferroelectric behaviour was found below 216 K [1–5]. In BP and BPI as well as in the respective deuterated compounds DBP and DBPI, the PO_4 and PO_3 tetrahedra are linked by the hydrogen bonds O_4–H_{13}–O_4 and O_6–H_{15}–O_6, thus forming quasi-one-dimensional zigzag chains along the crystallographic *b*-axis [3]. The two almost isostructural compounds form solid solutions at any concentrations [2]. In these mixed

0953-8984/99/061575+14$19.50

crystals, DBP and DBPI molecules are supposed to be arranged in the chains in a statistical manner, according to their relative occurrence.

Pure (non-mixed) BP and BPI, as well as DBP and DBPI, have been studied by different techniques. The investigation of symmetry and structural changes in relation to the phase transitions by x-ray, dielectric and magnetic resonance techniques revealed details of the static and dynamic properties of the protons in the hydrogen bonds [4–8]. By means of ^{2}H nuclear magnetic resonance (NMR) spectroscopy carried out on the deuterated compounds DBP and DBPI [9–11], the high-temperature phase transition was characterized as of order–disorder type, and the chemical exchange processes were quantitatively analysed by means of two-dimensional ^{2}H NMR exchange spectroscopy.

The study of the mixed-crystal system $DBP_{1-x}DBPI_x$ is especially challenging because of the competing ferroelectric and antiferroelectric interactions. Dielectric investigations were focused on the glass behaviour at low temperatures [12] and provided information on the relaxational and electrical conductivity properties. So far, no NMR investigations have been reported on this system. However, the use of quadrupole-perturbed one-dimensional ^{2}H NMR spectroscopy and—in particular—two-dimensional ^{2}H NMR exchange spectroscopy do look very promising as regards elucidating the details of the hydrogen dynamics. Such investigations are also expected to give new insight into the discrepancy between the higher rates of chemical exchange and lower electrical conductivity (DBP)—and vice versa (DBPI)—recently observed.

Therefore, taking advantage of these powerful NMR spectroscopic techniques, the scope of this paper as regards the system $DBP_{1-x}DBPI_x$ is as follows:

(a) An interpretation of the ^{2}H NMR spectra is achieved by attributing *all* spectral line doublets to their respective deuterium lattice sites by means of the measured rotation patterns. In this process it will be possible to distinguish between DBP and DBPI molecules in the same crystallographic chain spectroscopically.
(b) From the temperature variation of the ^{2}H NMR line shape, the dependency of the high-temperature phase transition on the phosphite concentration x will be derived. To account for this behaviour a theoretical model is suggested, which underlines the antiferrodistortive character of the transition.
(c) The deuterons taking part in processes of chemical exchange between several hydrogen bridges will be identified from the temperature dependencies of the 1D spectra. The qualitative findings on the exchange processes are refined by two-dimensional ^{2}H NMR investigations, resulting in the statement that it can also be proven that there are processes of exchange between different (DBP and DBPI) molecules in the crystallographic chains.

The specifications of the local deuterium lattice sites for $DBP_{1-x}DBPI_x$ are shown for a sequence of one DBP and two DBPI molecules in figure 1. The betaine molecules are arranged approximately perpendicularly to the chains and are connected to the phosphate and phosphite tetrahedra by two hydrogen bridges (O_5–H_{14}–O_1 and O_2–H_{12}–O_3) and one hydrogen bond (O_2–H_{12}–O_3), respectively [2]. In DBPI the fourth deuteron is directly bound to the phosphorus atom (P–H_{14}).

2. Experimental procedure

$DBP_{1-x}DBPI_x$ crystals were grown by controlled evaporation from D_2O solution containing betaine as well as H_3PO_3 and H_3PO_4. In this process not only a deuteration of the bridging atoms, but also, partially, one in the methylene groups of the betaine molecules was achieved. The phosphite concentrations x which are given for the $DBP_{1-x}DBPI_x$ crystals in this work are the nominal ones corresponding to x in the solution. For the NMR spectroscopy the

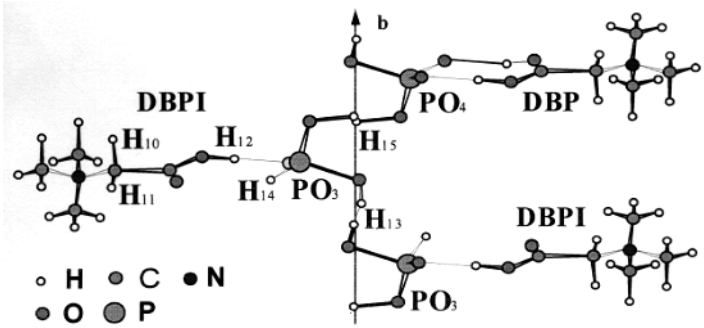

Figure 1. The structure of $DBP_{1-x}DBPI_x$ in the antiferrodistortive phase. A sequence of one DBP and two DBPI molecules is shown. The deuterated lattice sites are indicated for one formula unit according to [3].

same crystal samples were used as for the dielectric investigations, in order to facilitate the comparison of the results.

^{2}H NMR measurements were run at a resonance frequency of 46.073 MHz using a BRUKER MSL 300 NMR spectrometer. An excitation of the complete 1D spectrum was achieved with a pulse duration of 2.5 μs. A quadrupole spin–echo sequence with a pulse distance of 20 μs was used to avoid the influence of the dead time. Furthermore, proton decoupling was applied to suppress the broadening of the ^{2}H NMR lines due to dipolar interaction between the deuterons and the remaining protons. The repetition time was chosen between 5 s and 60 s depending on the temperature. For purposes of calibration, deuterated phosphorous acid was used.

Two-dimensional ^{2}H NMR exchange experiments were carried out, applying the echo sequence $(\pi/2)_x$–t_1–$(\pi/2)_{-x}$–τ_m–$(\pi/2)_x$–τ–$(\pi/2)_y$–τ–t_2. The values t_1, t_2, τ and τ_m denote the evolution time, acquisition time, pulse distance and mixing time, respectively. A duration of 20 μs was chosen for τ. 512 and 180 data points were acquired in the t_2- and t_1-directions, respectively, at a dwell time of 2 μs.

3. Results and discussion

3.1. Interpretation of the ^2H NMR spectra and assignment to the deuterium lattice sites

First, in order to interpret the ^{2}H NMR spectra of the system $DBP_{1-x}DBPI_x$, the number of lines appearing and their intensity relations have to be understood. For this purpose, rotation patterns of the spectra for $DBP_{0.3}DBPI_{0.7}$, $DBP_{0.15}DBPI_{0.85}$ and $DBP_{0.85}DBPI_{0.15}$ were measured in the antiferrodistortive phase at 300 K. In principle, the experimental basis for the determination of the EFG tensor elements (with the help of which the lines are assigned to lattice sites) is the measurement of the line splitting $\nu_2 - \nu_1$ between the two lines of a ^{2}H NMR doublet, which is proportional to the tensor element V_{zz} in the laboratory frame. The tensor elements in the crystallographic axes system can be determined from the experiment when the crystals are rotated around different crystal axes (in the *a*-, *b*- and *c*-directions) and if the rotation patterns are analysed by using the well-known Volkoff [13] formalism, which relates the tensor elements in the crystal frame to the line splitting measured.

However, the ^{2}H NMR spectra of $DBP_{1-x}DBPI_x$ show numerous line doublets with linewidths up to several kHz. A typical example is given in figure 2 for the case of $DBP_{0.3}DBPI_{0.7}$ for the rotation around the crystallographic *b*-direction. Seven line pairs are resolved in

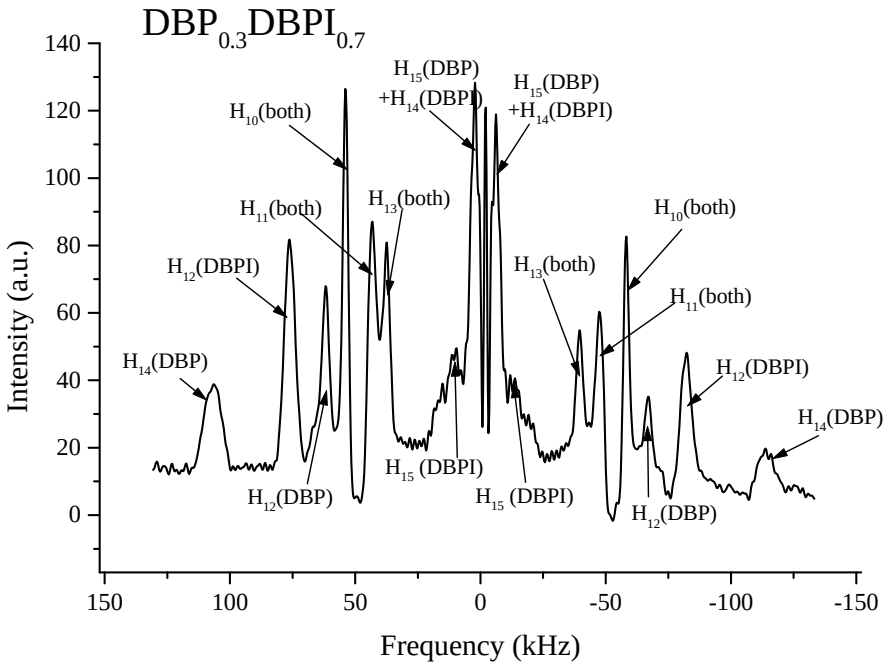

Figure 2. Typical ^{2}H NMR spectra of $DBP_{0.3}DBPI_{0.7}$ at a temperature $T = 300$ K with indications of the assignment of the ^{2}H NMR doublets to the local deuterium sites.

this rather favourable orientation (the assignment of deuterons, explained later, is already indicated). For other crystal orientations the line overlap is far more pronounced, and for rotations around the *a*- and *c*-axis, due to symmetry properties [9], a twofold number of lines is observed. The measured rotation pattern for $DBP_{0.3}DBPI_{0.7}$ for a rotation around the crystallographic *b*-axis is shown in figure 3 (full circles). Without further help, it is very difficult to follow all line courses in this pattern. Due to the increased number of lines and their overlap for rotations around the crystallographic *a*- and *c*-directions, it is even more complicated to group the measured line separations to the respective lines. As regards the sharp line observed for some crystals (e.g. in figure 2) at the resonance frequency, all indications point to residual deuterated water, as no angular dependence occurs and the line vanishes below $\approx$230 K.

To answer the question of whether the rotation patterns of $DBP_{0.3}DBPI_{0.7}$ are similar to those of DBP and DBPI or whether 'mixed' lines occur, it was inevitable that we made use of the knowledge that we have on pure DBP and DBPI [9, 10]. Therefore the overlay of the rotation patterns of the two pure substances is added in figure 3, where the fits of the respective rotations are displayed as full (DBP) and dashed (DBPI) curves. In the region between $\approx 80^\circ$ and 160°, both sets of fitting curves are given to illustrate the fit of all of the measured $DBP_{0.3}DBPI_{0.7}$ line separations; outside of this region, only one set is shown of each. As can be seen from this figure, the measured rotation pattern for $DBP_{0.3}DBPI_{0.7}$ can be fully understood by means of this approach. Apparently, for this rotation, all lines detected for $DBP_{0.3}DBPI_{0.7}$ correspond, within the resolvable linewidth, to lines of either pure DBP or pure DBPI. Thus, for this rotation pattern of $DBP_{0.3}DBPI_{0.7}$ we observe a superposition of the respective lines from the patterns of the pure substances. The patterns for the rotations around the crystallographic *a*- and *c*-directions (not shown here) could also be analysed by using this relationship to pure DBP and DBPI. From this correspondence of ^{2}H NMR lines

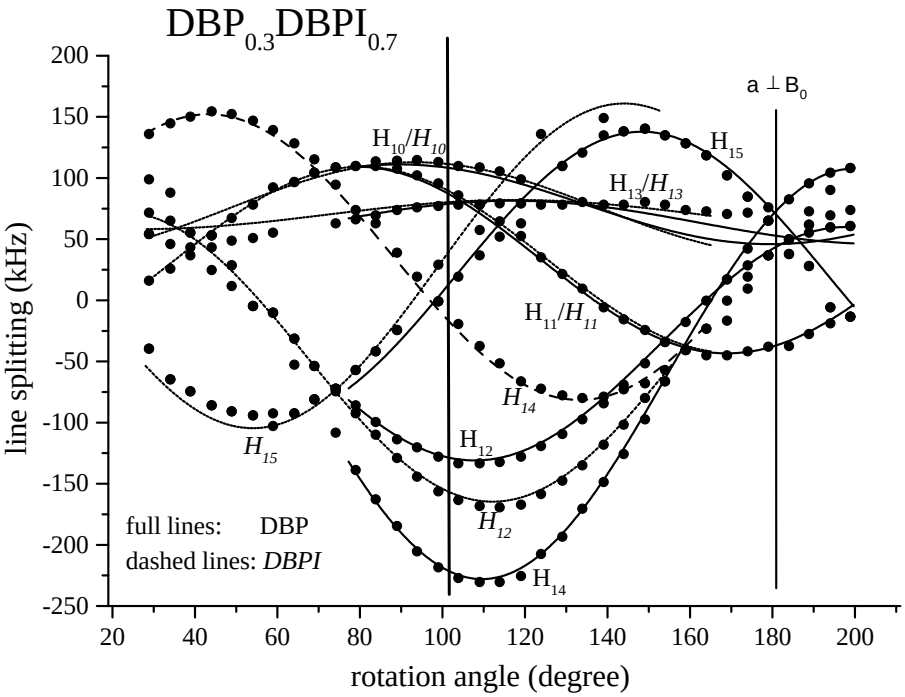

Figure 3. The rotation pattern of the angular dependence of the quadrupolar line splitting for $DBP_{0.3}DBPI_{0.7}$ in the antiferrodistortive phase for a rotation around the crystallographic *b*-direction. The *a*-axis is parallel to the external field at the angle 180°. Dots indicate the measured line separations for $DBP_{0.3}DBPI_{0.7}$; full and dashed curves show fits made on the basis of the fits for pure DBP and DBPI, respectively. The straight line at ≈102° indicates the orientation for the 2D studies.

for *all three* rotations, it follows immediately that the respective deuterium lattice sites have, within the experimental error, the same EFG tensors as the sites in pure DBP and DBPI [10]. This finding is not surprising if one assumes the EFG tensor to be a local quantity, i.e. that the local environment of the deuterons is not significantly changed when DBP molecules are built into DBPI chains and vice versa. Moreover, the assignment of the ^2H NMR lines of $DBP_{0.3}DBPI_{0.7}$ to local deuterium lattice sites with the help of the EFG tensors is achieved as indicated in figure 2, since the same tensors are assigned to the same sites as in pure DBP and DBPI. There, the assignment had been achieved using the relationships between the directions of the principal EFG components and those of the hydrogen bridges, as described in [9, 10].

The decisive difference in the spectra for other representatives of the mixed-crystal system consists in the smaller ($DBP_{0.15}DBPI_{0.85}$ and $DBP_{0.85}DBP_{0.15}$) or larger ($DBP_{0.4}DBPI_{0.6}$) linewidths of the ^2H NMR lines, whereas the line separations and their angular dependence are similar to those of $DBP_{0.3}DBPI_{0.7}$. The rotation patterns could therefore be explained in the same way as described above. For all of the mixed crystals studied, no experimentally detectable deviations of the EFG tensors towards those of the pure crystals were found.

The assignment of the ^2H NMR lines to the lattice sites for all of the mixed crystals was additionally confirmed by evaluating the intensity of the relevant lines. According to the respective phosphite concentration x for different $DBP_{1-x}DBPI_x$ crystals, the intensity of the lines assigned to deuterons in DBPI molecules increases or decreases, whereas lines

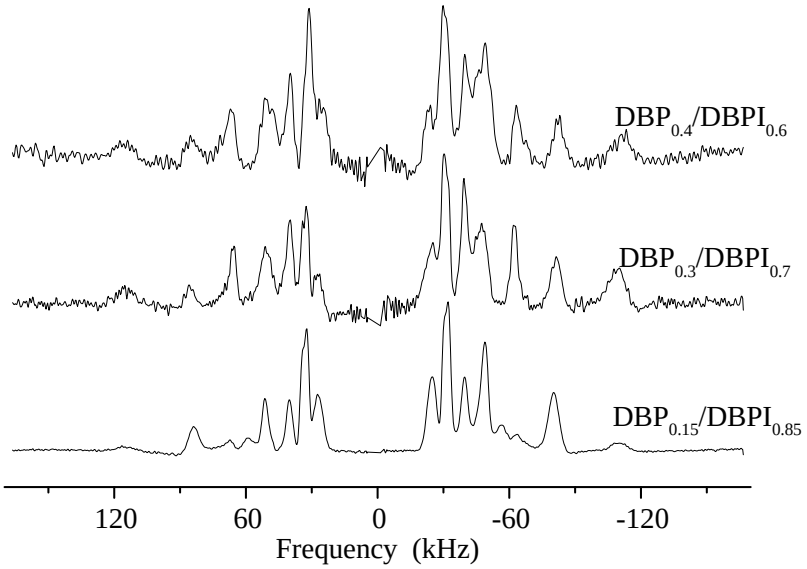

Figure 4. Comparison of ^{2}H NMR spectra for the phosphite concentrations $x = 0.85$, 0.7 and 0.6 in a selected orientation. Note the changes in linewidth, intensity and resolution.

assigned to deuterons in DBP molecules show characteristic intensity changes in the opposite direction. Figure 4 illustrates the change of intensity and linewidth (as well as resolution) of the ^{2}H NMR lines for different values of x in the same selected orientation. Although the intensity relations slightly deviate from the expected ratio $(1-x)/x$ for some $DBP_{1-x}DBPI_x$ crystals, the assignment of all ^{2}H NMR lines as described above is fully consistent with their characterization as lines of DBP or DBPI molecules on the basis of their intensities. The deviations of experimentally measured and theoretically calculated intensity ratios are not simply due to experimental factors (i.e. unequal excitation etc); differences in the phosphite percentage x between the solution and grown crystals as reported in [6] have also to be taken into account.

For all of the $DBP_{1-x}DBPI_x$ mixed crystals studied, the rotation patterns could be explained as superpositions of the rotation patterns of pure DBP and DBPI. All lines could be interpreted by assigning them to deuterons in DBP or DBPI molecules (in accordance with the relative intensities) in the chains of the mixed crystals. Hence, the EFG tensors as local quantities are not changed, and the rotation patterns appear as (weighted) averages of those of pure DBP and DBPI. As a crucial consequence of this, different molecules (i.e. DBP and DBPI molecules) in the same chain of $DBP_{1-x}DBPI_x$ are *spectroscopically distinguishable*.

When carefully considering the chain structure of $DBP_{1-x}DBPI_x$, however, the question arises of whether for the deuterons H_{13} and H_{15} intermolecular sites should be detectable. According to figure 1, for these deuterons three possible sites should exist: sites between two DBP molecules, between two DBPI molecules and between a DBP and a DBPI molecule, whereas for the deuterons H_{12} and H_{14} (as well as for the CD_2 groups), only sites within DBP or DBPI molecules exist. The experimental response consists in the finding of only one line belonging to H_{13} and two lines belonging to H_{15} (compare figure 2). In order to explain this, it is again very instructive to look at the superimposed lines from the rotation patterns of pure DBP and DBPI in figure 3. It is obvious that the H_{13} lines from DBP and DBPI are almost identical and that both lines for H_{15} have a biggest separation of at most 25 kHz. Therefore,

in the mixed crystals for H_{13}, always only one line is detected, and for H_{15}, two lines close to each other are found, where no decision is possible as regards whether one belongs to an intermolecular lattice site. Moreover, this also implies that the question of possible cluster formation in the chains cannot be answered on the basis of the experiments. It is not possible to distinguish between two H_{15} lines, corresponding to a regular arrangement of DBP and DBPI molecules, and three lines, implying clusters of DBP and DBPI molecules H_{15}, due to the overlap and the linewidth of several kHz.

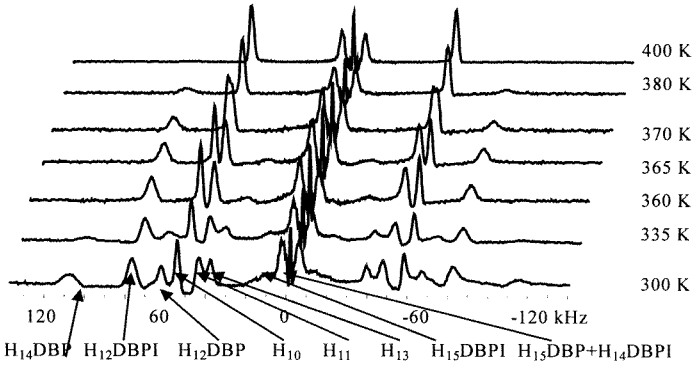

Figure 5. The temperature dependence of the quadrupolar line splitting of $DBP_{0.3}DBPI_{0.7}$ in an orientation where the crystallographic *b*-axis is perpendicular to the external magnetic field and the angle between the field and the *a*-axis is $\approx 104^\circ$. For the spectrum at 300 K, the deuteron positions are labelled.

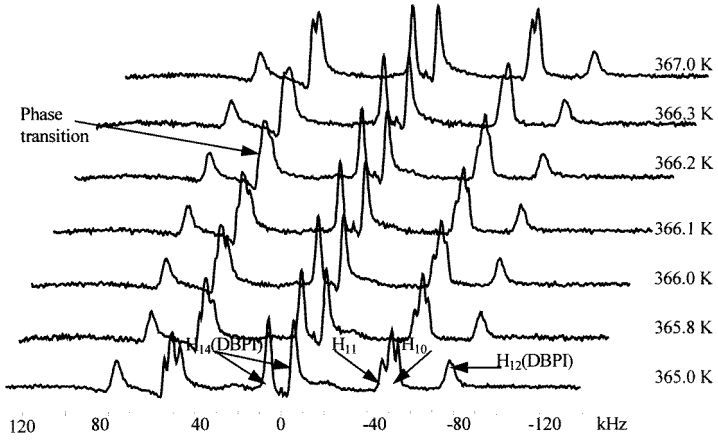

Figure 6. The temperature dependence of the quadrupolar line splitting of $DBP_{0.15}DBPI_{0.85}$ (for the same orientation as for figure 5) in the region 365 K to 367 K. The merging of the H_{10} and H_{11} lines at the phase transition point is indicated.

3.2. The temperature dependence of the spectra and phase transitions

Measurements of the temperature dependence of the quadrupolar line splittings were carried out over the temperature range from 90 K to 400 K in order to interpret the characteristic frequency and line-shape changes. For these measurements, suitable crystal orientations with the best

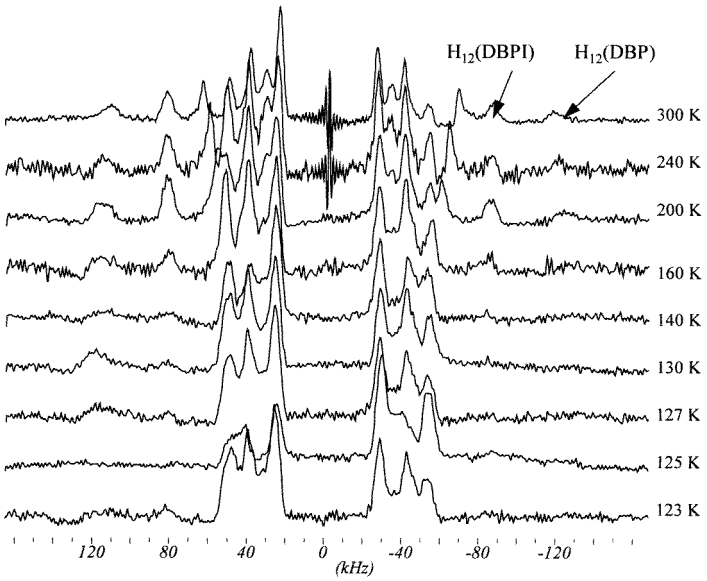

Figure 7. The temperature dependence of the quadrupolar line splitting of $DBP_{0.3}DBPI_{0.7}$ in the region from 123 K to 300 K.

possible resolution of the ^{2}H NMR lines were chosen. Typical spectra and their dependence on the temperature T are displayed in figures 5 to 7 for 300 K $< T <$ 400 K ($DBP_{0.3}DBPI_{0.7}$), 365 K $< T <$ 367 K ($DBP_{0.15}DBPI_{0.85}$) and 123 K $< T <$ 300 K ($DBP_{0.3}DBPI_{0.7}$). All of the selected spectra shown here were measured for orientations where the crystallographic *b*-axis is perpendicular to the magnetic field and the angle between the magnetic field and the *a*-axis is approximately 102°, as indicated by the vertical line in figure 3. Temperature dependencies were also acquired for $DBP_{0.4}DBPI_{0.6}$ and $DBP_{0.85}DBPI_{0.15}$. In the next sections we shall discuss the different phenomena which may be inferred from these spectra.

3.2.1. The high-temperature phase transition: measurements. First, the high-temperature phase transition from the antiferrodistortive (afd) to the paraelectric (pe) phase can be determined from two indications. The number of line pairs is reduced above the phase transition, which is apparent from figure 5, where the deuteron line doublets are labelled for $T = 300$ K, and figure 6. Line pairs arising from the CD_2 groups merge into one line pair above the phase transition temperature, where the low-temperature positions are symmetric with respect to the frequency observed above the transition. The number of lines observed is consistent with the symmetry properties (space group $P2_1/m$ in the pe phase), as discussed in detail for pure DBP and DBPI [9, 10]. Besides the number of ^{2}H lines observed above and below T_{C1}, the soft-mode behaviour of the spin–lattice relaxation time of the deuterons also confirms the presence of a phase transition for all of the $DBP_{1-x}DBPI_x$ crystals studied at this point. The high-temperature phase transition point T_{C1}, for which insufficient data from dielectric or ESR spectroscopy are available, could be determined for further selected representatives of the system $DBP_{1-x}DBPI_x$ by carefully inspecting the respective spectra which were acquired in steps of 0.1 K. In figure 6 the spectra set for $DBP_{0.15}DBPI_{0.85}$ is shown from which one can appreciate the sensitive changes of the H_{10} and H_{11} line shape and position even for temperature changes of only 0.1 K. For the phase transition temperature

T_{C1} a (non-calibrated) value of 366.2 K can be inferred from the merging of the H_{10} and H_{11} lines at ≈48 kHz. The H_{14}(DBPI) lines (not exchanging) and H_{12}(DBPI) lines (not completely broadened yet) are unaffected by the phase transition.

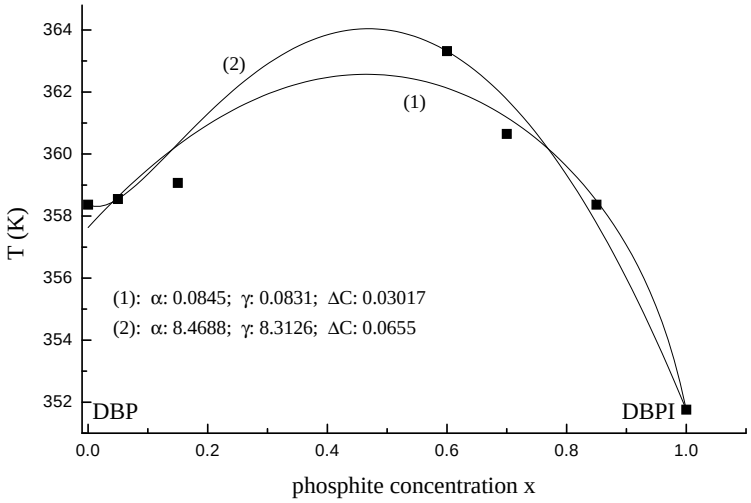

Figure 8. The phase transition temperature T_{C1} as a function of the phosphite concentration x for different representatives of the system $DBP_{1-x}DBPI_x$. The experimental data (dots) are fitted using two parameter sets of our model.

Consequently, a phase diagram in the sense of a diagram showing the dependence of the high-temperature phase transition on the degree of mixing (the phosphite concentration x) can be obtained, when the T_{C1}-values are read from the respective spectra sets (not shown here). The result is shown in figure 8, where the points represent the experimental T_{C1}-data. The temperature given there will be calibrated more exactly by means of ultrasonic measurements on DBPI [14], which allow a precise determination of T_{C1}. From figure 8 it follows that the difference in T_{C1}-value between pure DBP and DBPI is only ≈7 K, indicating a slight deviation from the expected value of 10 K [1, 2]. More interesting, however, is the fact that we do not find a linear dependence of T_{C1} on x, but T_{C1} exhibits a maximum near the middle of the mixed-crystal row (at 363.3 K for $x = 0.6$ in figure 8). Unfortunately, at present no statement can be made for values in the range $0.15 < x < 0.6$ (in particular, the supposed maximum at $x = 0.5$ could not be checked), since no crystals were available for the NMR measurements. From the detected maximum, the phase transition temperature T_{C1} decreases to 358.4 K (pure DBP) and 351.7 K (pure DBPI), with the decrease towards pure DBPI being steeper.

3.2.2. The high-temperature phase transition: theoretical explanation. To elucidate, from this point of view, the observed concentration dependence of the afd phase transition temperature T_{C1} for the system $DBP_{1-x}DBPI_x$, it is necessary to consider the lattice dynamics of the system. This is quite a difficult problem practically but, as is well known, the essential microscopic features of the system undergoing a structural phase transition can be explained within the framework of the model of coupled anharmonic oscillators. Their parameters can, in principle, be calculated from the exact lattice dynamics (see e.g. the well-known monographs of Lines and Glass [15] and Bruce and Cowley [16]).

In the order–disorder limit, which we will consider, this model is equivalent to the Ising model [16], and the phase transition temperature of a pure system in this model is determined

by means of the following relationship [16]:

$$T_{C1} = 4dC\frac{A}{B}. \tag{1}$$

Here A and B are the parameters of the single-site double-minimum potential, whereas C describes the coupling constant for the nearest-neighbour unit cells. The dimensionality of the vibrating system is characterized by d.

Our system under consideration is a two-component solid solution, and therefore there are two sorts of unit cell in the crystal. This implies that the microscopic model of coupled anharmonic oscillators is now characterized by two sorts of single-site double-minimum potential with the parameters A_α and B_α ($\alpha = 1, 2$) as well as the coupling constants $C_{\alpha\beta}$ ($\alpha, \beta = 1, 2$), where $C_{\alpha\beta} = C_{\beta\alpha}$ because of the symmetry of the interaction. Therefore it represents a dynamic system of two different stochastic disordered anharmonic oscillators, located at each lattice site and coupled by the corresponding interaction. Now the true potential at a particular lattice site is approximated by the averaged potential at that site (the virtual-crystal approximation; see e.g. Elliott *et al* [17]).

Using this approximation, with x being the concentration of component 1 (DBPI in our case), we are able to calculate the static and dynamic properties of the disordered system with the same exactness as for the pure system (equation (1)). If we measure A_2 and B_2 in units of A_1 and B_1 ($A_2 = \gamma A_1$ and $B_2 = \alpha B_1$), respectively, and assume that $C_{11} \approx C_{22}$, then we finally find for this concentration dependence the explicit expression

$$T_{C1}(x) = T_{C1}(x = 1)\frac{\left[(1-x)/\gamma\right] + x}{[(1-x)/\alpha] + x}\left[1 + 2x(1-x)\,\Delta C\right] \tag{2}$$

with

$$\Delta C = \frac{C_{12} - C_{11}}{C_{11}}$$

where x is the concentration of component 1 (DBPI in our case). Details of the considerations used to obtain this equation, together with a different, more general, theoretical approach which allows the exact derivation of equation (2), are given in a forthcoming paper [18].

Equation (2) contains the three parameters α, γ and ΔC, whereas the ratio

$$\gamma/\alpha = T_C(x = 0)/T_C(x = 1)$$

is given by the experiment and equals 0.981 55. The result of the fit of the measured T_{C1}-values to the model of equation (2) can be estimated from figure 8, where two fitting curves are given. Curve (1) was obtained by fitting all three parameters to the experimental data points. An even better approximation for the T_{C1}-values is represented by curve (2). This was obtained by determining the two remaining free parameters γ and ΔC by inserting the values for $x_1 = 0.6$ and $x_2 = 0.05$ into equation (2) and solving the resulting equation system for γ and ΔC. In either case, the decisive common property is the fact that a qualitative description is accomplished in the sense that from our model it necessarily follows that T_{C1} must go through a maximum. Thus, from our model, in accordance with the experiment, a non-linear dependence of T_{C1} on x with a maximum at or near the value $x = 0.5$ can be derived. For a more detailed discussion of the physical content of this behaviour, i.e. the occurrence of a dependence of the long-range order on the value of the coupling constant, further measurements will be necessary, in combination with the different theoretical approach mentioned above.

3.2.3. Low-temperature behaviour. The temperature dependence of the ^{2}H NMR spectra in the temperature range between ≈90 K and 300 K was studied for $DBP_{0.3}DBPI_{0.7}$ and

$DBP_{0.4}DBPI_{0.6}$, because these systems were expected to show the most significant changes. Although the present measurements are not sufficient for us to draw detailed conclusions, we shall indicate our preliminary observations. In figure 7 it can be seen that for $DBP_{0.3}DBPI_{0.7}$ several lines broaden and merge when the temperature is decreased (the assignment of the lines for $T = 300$ K corresponds to those of figure 5). A slight frequency shift, being most clearly visible for H_{12}(DBP) and H_{12}(DBPI), towards lower line separations occurs, and it can be stated that there is an increasing line overlap below temperatures of approximately 150 K. However, from the available measurements, the phase transition from the afd to the low-temperature phase, where antiferroelectric and ferroelectric interactions compete, cannot be localized.

An interesting fact is that preliminary results for $DBP_{0.4}DBPI_{0.6}$ indicate an *increasing* line separation at temperatures around 90 K again. This can be considered to be an indication that the freezing of deuterons, which possibly can be set into relation to a transition to glassy behaviour, is detectable by means of ^2H NMR. A further consideration of these aspects seems not to be appropriate here and is therefore left for more detailed investigations.

3.3. Chemical exchange processes

3.3.1. 1D spectra and chemical exchange. The second significant phenomenon which can be inferred from the temperature dependence of the ^2H NMR spectra (figure 5) is a broadening and overlapping of the ^2H NMR lines originating from the bridging deuterons (except the H_{14} line of DBPI) if the temperature is increased above ≈330 K. These changes of line shape can be clearly attributed to chemical exchange processes which can be expected from having in mind the exchange phenomena observed in the pure compounds [19]. However, even at the highest temperatures measured (≈400 K) no averaged line pair belonging to the bridging deuterons can be observed. These findings, demonstrated here for the sample $DBP_{0.3}DBPI_{0.7}$, also apply to the other mixed crystals which were investigated. Therefore the following considerations for the qualitative exchange behaviour refer to the whole $DBP_{1-x}DBPI_x$ system.

An important conclusion which can be drawn here consists in the fact that both the ^2H NMR lines originating from DBP molecules (H_{12}, H_{13}, H_{14} and H_{15}) and those originating from DBPI molecules (H_{12}, H_{13} and H_{15}) apparently take part in the exchange process (compare figure 5). Since we are able to distinguish between DBP and DBPI molecules (or intermolecular sites as discussed above) in the chains of the system $DBP_{1-x}DBPI_x$ spectroscopically, this observation constitutes an important step towards evidence of exchange processes along the chains. In agreement with the studies on pure DBPI, the line H_{14}(DBPI) does not show the line-shape variations characteristic for exchange processes. Thus, the deuteron H_{14}, which is directly bound to the phosphorus atom in the PO_3 tetrahedra in the system $DBP_{1-x}DBPI_x$ as well, does not take part in the chemical exchange.

In order to study the dynamics of this exchange process and to find explanations for the different exchange rates in pure DBP and DBPI, similar considerations to those for the pure substances in [19] on the calculation of an absorption spectrum are necessary [20]. For the system $DBP_{1-x}DBPI_x$ we find a total of seven (four of DBP and three of DBPI) deuterium sites taking part in the exchange processes. Therefore the rate matrix composed of the transition probabilities p_{ij} between the sites i and j and describing the dynamics of the exchange process is of order 7×7. Moreover, the relative occupation numbers n_{ij} are now to be obtained as products of the percentage (concentration) in the mixture and a factor of 1 or 0.5 indicating whether a deuteron belongs entirely or only half belongs to the respective molecule. For the pure substances DBP and DBPI, the simple assumption about the exchange process had been adopted that all bridging deuterium atoms exchange with the same temperature-dependent

exchange rate p, and a difference in the rates of approximately two orders of magnitude was found [19]. Due to this difference, for the system $DBP_{1-x}DBPI_x$, for the interpretation of the line-shape variations versus temperature, this simple assumption has to be dropped from the outset.

On the basis of the one-dimensional measurements, no differentiation as regards the deuterium exchange among the different sites with different p_{ij} is possible. For a first approximation of the rates of the observed exchange processes in $DBP_{0.3}DBPI_{0.7}$, from the temperature dependence of the one-dimensional ^{2}H NMR spectra, comparison between the measured $DBP_{1-x}DBPI_x$ spectra and the results for pure DBP and DBPI is used. This shows that for $T \leqslant 330$ K the lines are not broadened by exchange processes and that the exchange rates are smaller than 0.5 kHz. Above ≈390 K all bridging deuterium atoms except H_{14}(DBPI) participate in the fast exchange and the exchange rates are greater than 200 kHz. Similar considerations can be pursued for $DBP_{0.15}DBPI_{0.85}$, $DBP_{0.4}DBPI_{0.6}$, $DBP_{0.85}DBPI_{0.15}$ and $DBP_{0.95}DBPI_{0.05}$.

3.3.2. Two-dimensional exchange experiments. Although from the present one-dimensional ^{2}H NMR investigations we have strong hints that all bridging deuterons except H_{14}(DBPI) are involved in the exchange process, the shortcoming of these studies is the lack of differentiation as regards the deuterium exchange among the different sites. On the basis of this line-shape analysis, it is not possible to analyse the exchange processes in more detail. In order to determine exchange rates and activation energies, measurements of 2D ^{2}H NMR exchange spectra are suggested. However, compared to the case for the studies on the pure substances, a number of difficulties occur.

A typical 2D ^{2}H NMR exchange spectrum of $DBP_{0.3}DBPI_{0.7}$ measured in the antiferrodistortive phase at a temperature of 318 K is shown in figure 9. For the 2D exchange experiments, an orientation of the crystal was chosen for which the crystallographic *b*-axis is perpendicular to the external magnetic field, and a maximum number of resolved ^{2}H NMR lines is achieved. The assignment of the deuterium lattice sites to the peaks is indicated for the lower left-hand quadrant of the symmetric 2D spectrum. As indicated in figure 9, eight resolved lines occur (it follows from the rotation patterns that no orientation with better resolution exists). The drawback of this orientation is the relatively large spectral width of 250 kHz, implying certain excitation problems.

First, it can be inferred from the occurrence of off-diagonal peaks in the ^{2}H NMR spectra that, at this temperature, processes of exchange between the bridging deuterons may already be observed. Off-diagonal peaks between H_{15}(DBPI), H_{13}(both), H_{12}(DBP) and H_{12}(DBPI) may be clearly found, and, if one inspects the respective spectral regions quite carefully, off-diagonal peaks connecting H_{15}(DBP) and H_{14}(DBP) to other peaks may also be discerned. The allegedly lower intensity of the latter cross-peaks, which makes the separation from the noise more difficult, should not be seen as an argument in support of less or no exchange between the respective deuterium sites. This situation is due instead to the relative intensity of only 30% for the lines H_{15}(DBP) and H_{14}(DBP), their linewidth and additional excitation problems for the line H_{14}(DBP) with a line separation of ≈225 kHz. Since we observe off-diagonal peaks between the deuterium atoms in *all types* of hydrogen bridge except H_{14}(DBPI), this is unquestionably an indication for an exchange also between different (DBP and DBPI molecules) in the chains of $DBP_{0.3}DBPI_{0.7}$. This is illustrated by the arrow in figure 9 at the cross-peak, which indicates exchange between the deuteron H_{12} in the DBP molecules and the deuteron H_{12} in the DBPI molecules. Hence, the deuterons are able to move along the chains in the *b*-direction, which is considered to be a possible mechanism for the ionic conductivity found in these crystals [21, 22]. On the basis of these findings, the estimation of an effective

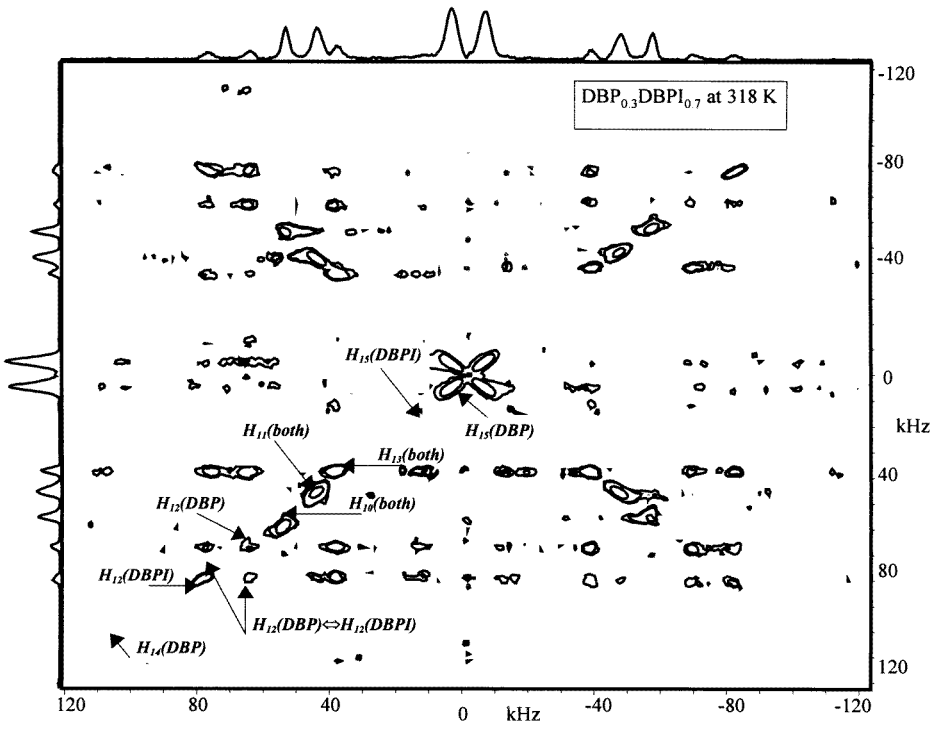

Figure 9. The 2D ^{2}H NMR spectrum of $DBP_{0.3}DBPI_{0.7}$ at a temperature of 318 K with a mixing time of 50 ms. The orientation (with the crystallographic *b*-axis perpendicular to the magnetic field) is indicated by the vertical line in figure 3. Diagonal and selected off-diagonal peaks are labelled.

charge-carrier density for the crystal $DBP_{0.3}DBPI_{0.7}$ [23] becomes more justified, because in particular the jumps in the chain direction, i.e. between DBP and DBPI molecules, contribute in this approach.

Secondly, we have to be aware that even in this rather favourable orientation the H_{15}(mix) and H_{14}(DBPI) peaks as well as the H_{13}(DBPI) and H_{13}(mix) peaks completely overlap and other peaks (such as H_{10} ones) partially overlap. This situation additionally complicates the quantitative analysis, which is already affected by the low intensities of the peaks outside a spectral width of approximately 120 kHz. A separation of the different exchange paths and their quantitative analysis is aimed for, in order to explain the different exchange rates found for pure DBP and DBPI [19]. Therefore, besides the measurement of mixing-time dependencies of the peak intensities, additional considerations concerning the treatment of the overlapping peaks are necessary. Further work on these aspects is in progress.

4. Summary

The quadrupole-perturbed ^{2}H NMR spectroscopy enables a selective study of the behaviour of the deuterium atoms in the hydrogen bridges and in the methylene groups of $DBP_{1-x}DBPI_x$ to be made. DBP and DBPI molecules in the one-dimensional chains can be distinguished spectroscopically. The high-temperature phase transition determined from the temperature dependence of the spectra shows a characteristic dependence on the degree of mixing. Our

suggested model describes this dependency, which is qualitatively in agreement with the afd character of the transition.

All bridging deuterium atoms (DBP and DBPI molecules, intermolecular sites) except H_{14}(DBPI) undergo a fast exchange process with rates greater than 200 kHz at temperatures above 380 K. Preliminary 2D ^{2}H NMR exchange experiments on $DBP_{0.3}DBPI_{0.7}$ give evidence for exchange processes *along* the one-dimensional chains. This observation is particularly important as regards the explanation of electrical conductivity phenomena. Further measurements, also on $DBP_{0.15}DBPI_{0.85}$ and $DBP_{0.85}DBPI_{0.15}$, are in progress to follow the different dynamics of the bridging deuterons.

Acknowledgments

We are grateful to Dr A Klöpperpieper, Saarbrücken, for providing the $DBP_{1-x}DBPI_x$ crystals. Furthermore, the support of the Deutsche Forschungsgemeinschaft is gratefully acknowledged.

References

[1] Albers J, Klöpperpieper A, Rother H J and Ehses K H 1982 *Phys. Status Solidi* a **74** 553
[2] Albers J, Klöpperpieper A, Rother H J and Haussühl S 1988 *Ferroelectrics* **81** 27
[3] Schildkamp W and Spilker J 1984 *Z. Kristallogr.* **168** 159
[4] Hellenbrand K-H, Ehses K H and Krane H-G 1991 *Z. Kristallogr.* **195** 251
[5] Pöppl A, Völkel G, Metz H and Klöpperpieper A 1994 *Phys. Status Solidi* b **184** 471
[6] Santos M, Andrade L, Costa M, Chaves M, Almeida A, Klöpperpieper A and Albers J 1997 *Phys. Status Solidi* b **199** 351
[7] Bauch H, Böttcher R and Völkel G 1993 *Phys. Status Solidi* b **178** K39
[8] Bauch H, Böttcher R and Völkel G 1993 *Phys. Status Solidi* b **179** K41
[9] Freude P and Michel D 1995 *Ferroelectrics* **165** 329
[10] Freude P and Michel D 1996 *Phys. Status Solidi* b **195** 297
[11] Freude P, Michel D and Totz J 1998 *Ferroelectrics* **208+209** 93
[12] Hemberger J, Ries H, Loidl A and Böhmer R 1996 *Phys. Rev. Lett.* **76** 2330
[13] Volkoff G M, Petch H E and Smellie D W L 1951 *Phys. Rev.* **84** 602
[14] Samulionis V, Banys J, Völkel G and Klöpperpieper A 1999 *Phys. Status Solidi* a at press
[15] Lines M E and Glass A M 1977 *Principles and Application of Ferroelectrics and Related Material* (Oxford: Clarendon) chs I to III
[16] Bruce A D and Cowley R A 1981 *Structural Phase Transitions* (London: Taylor and Francis) ch III
[17] Elliott R J, Krumhansl J A and Leath P L 1974 *Rev. Mod. Phys.* **46** 465
[18] Braeter H, Totz J and Michel D 1999 in preparation
[19] Freude P, Totz J, Michel D and Arndt M 1998 *J. Phys.: Condens. Matter* **10** 429
[20] Abragam A 1961 *Principles of Nuclear Magnetism* (Oxford: Oxford University Press)
[21] Banys J, Klimm C, Völkel G, Böttcher R, Bauch H and Klöpperpieper A 1996 *J. Phys.: Condens. Matter* **8** L681
[22] Hutton S L, Fehst I, Böhmer R, Braune M, Mertz B, Lunkenheimer P and Loidl A 1991 *Phys. Rev. Lett.* **15** 1990
[23] Totz J, Michel D, Banys J and Klöpperpieper A 1998 *J. Phys.: Condens. Matter* **10** 9281